Determination of Ultrasonic Absorption and Velocity and the Derived Thermodynamic Properties of Pure and Binary Molten Salts

W. Fuchs and J. Richter

Institut für Physikalische Chemie der RWTH Aachen, Aachen

Z. Naturforsch. **39 a,** 1279 – 1290 (1984); received November 2, 1984

The absorption and velocity of ultrasonic waves in molten salts are studied with an improved pulse method, which allows an exact and immediate measurement of the runtime of the impulses and of the amplitude of the recorded signals.

The measurements are performed in the pure molten salts sodium nitrate, potassium nitrate, and silver nitrate as well as in the three binary mixtures of these salts in the temperature range between 430 K and 620 K at various compositions. All values are measured at 27.789 MHz, the resonance frequency of the quartz transducers being used.

From the ultrasonic velocity, together with the expansion coefficient and the specific heat capacity, the adiabatic compressibility, the adiabactic constant, and the Rao's constant have been calculated. From the ultrasonic absorption and velocity results the volume viscosity, which can be referred to the structural relaxation of the molecules in the fused salts investigated here.

1. Introduction

An acoustic wave in a medium is absorbed by various irreversible processes. Here a part of the acoustic energy is absorbed and dissipated by inner friction, heat conduction, thermal radiation, relaxational processes, and chemical reactions.

The well known classical theory, developed by Stokes [1] and Kirchhoff [2], only considers shear viscosity and heat conduction as causes for the absorption of sound. The other, above mentioned, effects can be summarized under the term "volume viscosity".

The experimental determination of the volume viscosity thus provides hints on processes of relaxation and chemical reactions, where the frequency of relaxation is higher than the frequency of the transmitted sound wave.

We assume that all quantities involved in the description of a plane sound wave are proportional to

$$\exp\left[i\,\omega\,(t - x/u) - \alpha\,x\right],$$

where x is the distance, t the time, $f = \omega/2\pi$ the frequency of the sound, u its velocity and α the coefficient of absorption of the amplitude. Then, in first approximation, i.e. if $\alpha\,u/\omega \ll 1$, one has

$$\alpha = \frac{\omega^2}{2\varrho_0\,u^3}\left[\frac{4}{3}\,\eta + \eta_v + \frac{\lambda\,(\gamma - 1)}{\tilde{C}_p}\right], \qquad (1)$$

where ϱ_0 is the density, η the shear viscosity, η_v the volume viscosity, λ the coefficient of heat conduction, $\tilde{C}_p$ the specific heat capacity at constant pressure and $\gamma = \tilde{C}_p/\tilde{C}_v$. Equation (1) is given and discussed in [3], Chapter XII, Equation (175). In molten salts, γ is close to unity, so that the last term in (1) can be neglected. The classical viscothermal theory of Stokes [1] and Kirchhoff [2] does not contain the term η_v. As difference of α to the classical coefficient of absorption results the value

$$\alpha - \alpha_{\text{class}} = \frac{\omega^2\,\eta_v}{2u^3\,\varrho_0}. \qquad (2)$$

2. Experimental

Among the known methods for the determination of sound absorption and sound velocity the pulse method was chosen since it is more convenient for measurements at high temperatures, because disturbing echos can be avoided, and no direct contact between the sound transducer and the melt is necessary.

The pulse methods have already been used for the determination of sound velocity and absorption at room temperature and up to 120 °C. In this temperature range the sound transducer can be immersed directly into the liquid [4, 5]. Andreae et al. [6] measured at higher pressures, where the

0340-4811 / 84 / 1200-1279 $ 01.30/0. – Please order a reprint rather than making your own copy.

sound was transmitted via quartz rods into the measuring device.

Ultrasonic measurements on molten salts were carried out by Richards et al. [7], Bockris et al. [8], Higgs and Litovitz [9], Sternberg and Vasilescu [10] and Marchisio et al. [11]. In these papers a variant of the pulse method was described, however, only measurements of the sound velocity were done. Higgs and Litovitz [9] also determined the sound absorption.

We adjusted the pulse method for the measurements in such a way that an exact determination of the amplitudes of the received pulses was possible [12]. From this measurement of the amplitude the sound absorption can be calculated.

The mechanical setup of the experiment is similar to Richards et al. [7] (Figure 1). The electronic part was completely redesigned to ensure an exact measurement of amplitudes.

The transmitting quartz is stimulated by an electrical burst, generated by the pulse generator and the pulse modulated signal generator. After passing through the delay rods and the measuring cell the sound pulse is received by the lower quartz. The

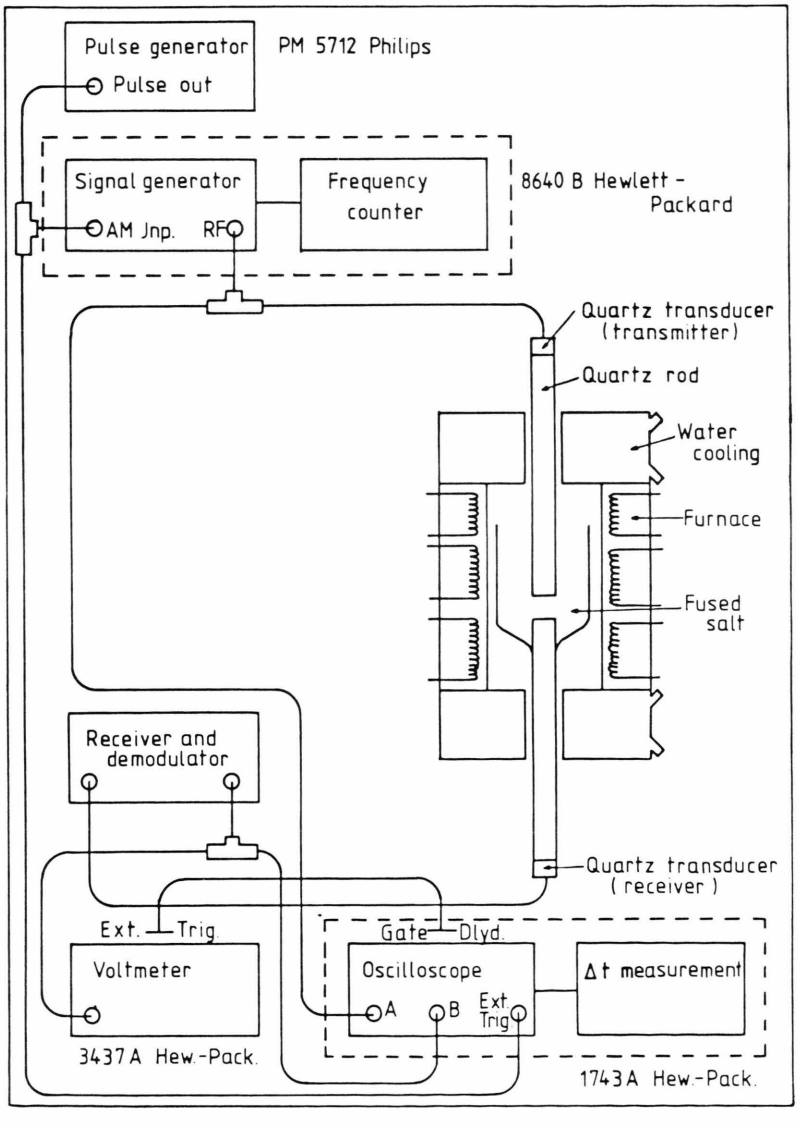

Fig. 1. Arrangement for the measurement of the ultrasonic absorption and velocity properties of molten salts.

received signal is amplified and demodulated, and the amplitude is recorded with the system voltmeter and the transit time with an oscilloscope.

The upper rod with the transmitting quartz is mounted in a micrometer drive mechanism (not shown in the figure). By electrically controlled stepper motors an exact positioning of the upper rod in increments of 0.1 μm is possible.

A Philips PM 5712 pulse generator is used for the generation of squarewave pulses and for controlling the timing of the whole electronic system. 100 pulses with a duration of about 2 μs are generated per second.

These pulses are sent over a coaxial cable to the AM input of the signal generator (Hewlett-Packard 8640 B) and modulate the carrier signal generated by this device. Furthermore these pulses trigger the oscilloscope for the time measurement.

The signal generator generates a burst with a frequency of 27.789 MHz, the resonance frequency of the used quartzes. The signal is of high spectral purity, constant amplitude and frequency.

On the side of the receiving quartz the signal is led to an amplifier and a demodulator. The electrical signal, which is sent off by the receiving quartz, is about 80 dB smaller than the original transmitted signal. To enable a measurement of amplitudes the received signal must at least be amplified to the fifth decimal power. For this purpose a special, low-noise broadband amplifier was developed and built. This amplifier allowed to work with very low transmitting energies of − 20 dBm. These low sound amplitudes come closest to the demands of the theory to keep as small as possible the disturbancies in the liquid caused by the sound wave.

The amplified and demodulated signal is led to the Hewlett-Packard 3437 A voltmeter as well as to the Hewlett-Packard 1743 A oscilloscope. The voltmeter is triggered by the "Gate Dlyd" exit of the oscilloscope, which enables to measure the height of the peak digitally.

Channel A of the oscilloscope is used to display the transmitted signal and channel B for the received signal. The built in time reference allows a digital measurement of the time difference between the two channels.

At the beginning of the sound absorption measurement the two quartz rods are moved to a distance larger than 1 mm and the transmitting level is adjusted so that the amplitude of the received signal is about 8 V after amplification. The once adjusted level of the transmitter must remain constant over the whole time of the measurement.

The upper quartz rod is now moved higher in some steps over the total distance of 20 mm. The peak heights of the directly passing signals are measured with the voltmeter, and an exponential curve fitting and an error analysis are performed.

Figure 2 shows on the left the experimental setup. In the middle a column diagram is assigned to it, in which the signal level in the different parts of the experiment is shown. At the transmitting quartz an electrical signal is applied which is taken to be 100%, corresponding to an absorption of zero decibel. The losses in the quartzes account to about 15 dB each, at the phase transition to about 7 dB, and in the quartz rods to 1 dB, so that the amplitude in the fused salt is only 1% of the initial one.

The sound wave is transformed in the receiving quartz into an electrical signal which is 80 dB lower. This means that the amplitude has decreased to 0.01%. The absorption to be measured in the fused salt (shaded area in Fig. 2) ranges from 0 to 5 dB, depending on distance and frequency of the sound wave, so that a change of the absorption from 75 dB down to 80 dB has to be measured. Therefore care must be taken to ensure the absolute constancy of

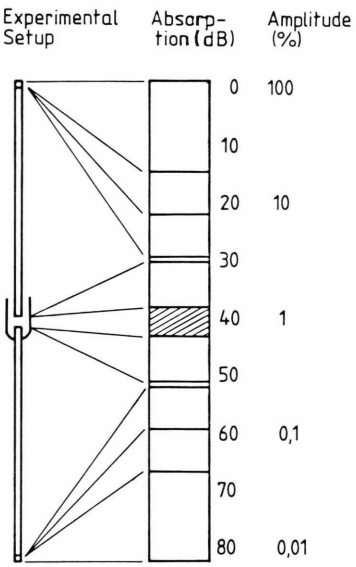

Fig. 2. Sound absorption in the different parts of the experimental setup.

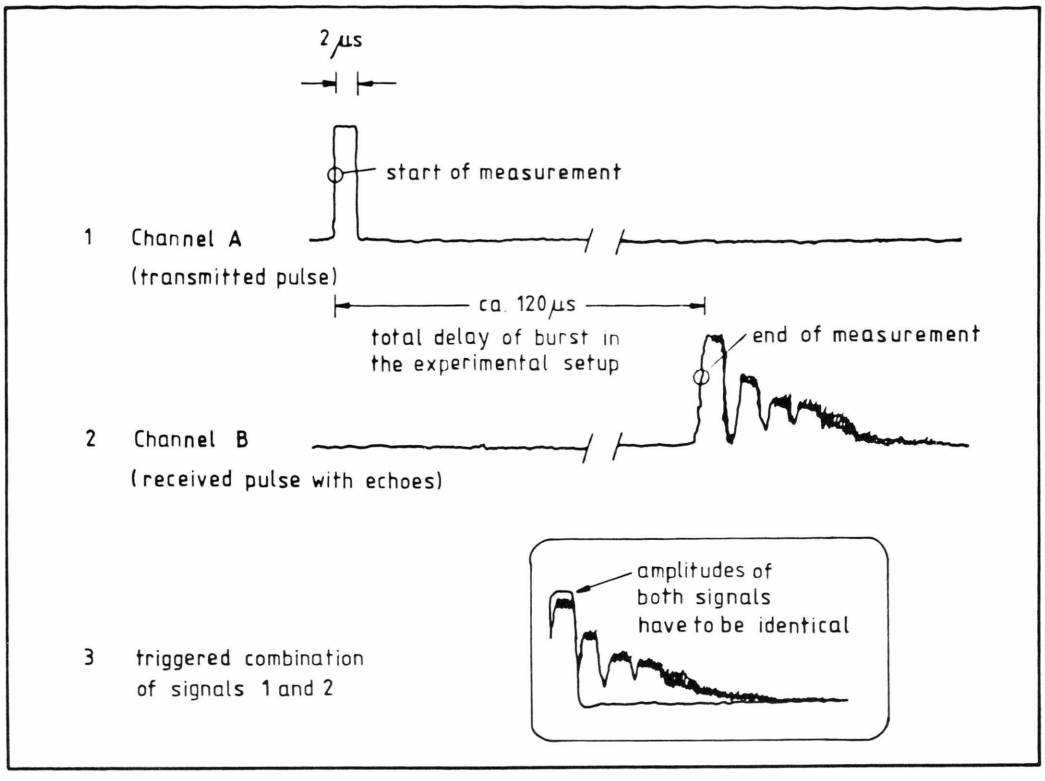

Fig. 3. Measurement of sound velocity.

the parasitic absorptions and the stability of the electronic device during the time of measurement.

For every distance x the damping, measured in dB and defined by

$$D_x = 20 \log (U_x / U_0) \tag{3}$$

with U_0 and U_x the respective amplitudes, is calculated. The absorption coefficient then results from the equation

$$\alpha = \frac{1}{20 \log e} \frac{D}{x}. \tag{4}$$

The principle of the sound velocity measurement is outlined in Figure 3. The oscilloscope is switched in such a way, that the transmitted and received signals appear simultaneously and are superposed on the screen. It is essential that the amplitudes of the transient pulse prior to and after the variation of the distance are the same. In Fig. 3 the starting point of the measurement is marked on the transmitted signal and the stopping point is marked on the received signal. The time between these two labels is measured with an accuracy of 10 ns. The distance between the two quartz rods is again varied with a micrometer drive mechanism in several steps over a total distance of 20 mm.

3. Sound Absorption

$NaNO_3 + AgNO_3$

In Fig. 4 the α values at 620 K are displayed. The error beams in this and all the following figures correspond to the 2σ-interval, i.e. a confidence interval of 95%.

The ultrasonic absorption shows a flat maximum at the mole fraction $x_{AgNO_3} = 0.6$. The absorptions of the pure components were measured by Higgs and Litovitz [9] and agree very well with the values of this work. The absorption coefficient is also known from Brillouin-scattering experiments, done by Knape [13]. The values of the scattering experiments are about 20% lower. This may indicate a relaxation frequency above the frequencies measured up to

now. α rises slowly in the measured temperature range with lower temperatures.

$KNO_3 + AgNO_3$

Figure 5 shows the ultrasonic absorption at 620 K depending on the composition. The absorption has a flat maximum at $x_{AgNO_3} = 0.35$. Towards the silver nitrate richer side ($x_{AgNO_3} > 0.5$) the absorption decays rapidly. The ultrasonic absorption of the two pure components has been measured by Higgs and Litovitz [9], whose values are in good accordance with the values in this work. For $AgNO_3$ the measured values are nearly identical, for KNO_3 the value of Higgs and Litovitz is 6% lower.

Because of the low melting point at the eutectic composition of the $KNO_3 + AgNO_3$ system it was possible to measure the temperature dependence of the absorption coefficient at this composition ($x_{AgNO_3} = 0.6$) over a range of 200 K. Here a clear rise of the ultrasonic absorption with lower temperatures can be observed (Figure 6).

$NaNO_3 + KNO_3$

The measured values of the ultrasonic absorption at 620 K are presented in Figure 7. Our values differ on the potassium rich side up to 40% from the values of Higgs and Litovitz. With some effort it is possible to link the measured values by a straight line within the 2σ-error range, which might also correspond to the values of Higgs and Litovitz. The limiting values, which have much smaller error ranges, are in agreement.

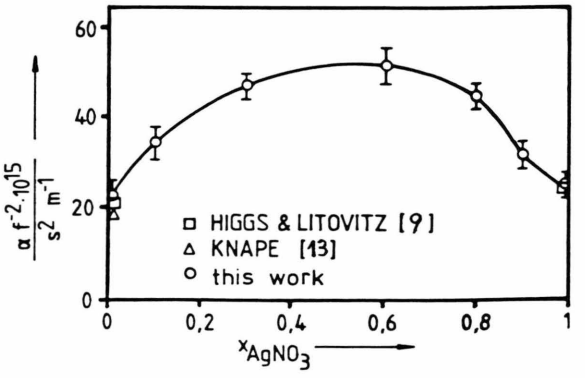

Fig. 4. $NaNO_3 + AgNO_3$: Sound absorption coefficients as a function of the mole fraction of silver nitrate at 620 K and 27.789 MHz.

4. Sound Velocity

$NaNO_3 + AgNO_3$

The measured values of the ultrasonic velocities are given in Table 1 depending on composition and temperature. The temperature dependence of the ultrasonic velocity at all compositions is nearly

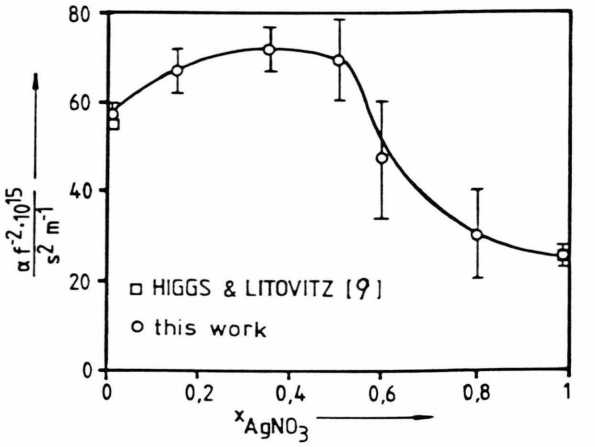

Fig. 5. $KNO_3 + AgNO_3$: Sound absorption coefficients as a function of the mole fraction of silver nitrate at 620 K and 27.789 MHz.

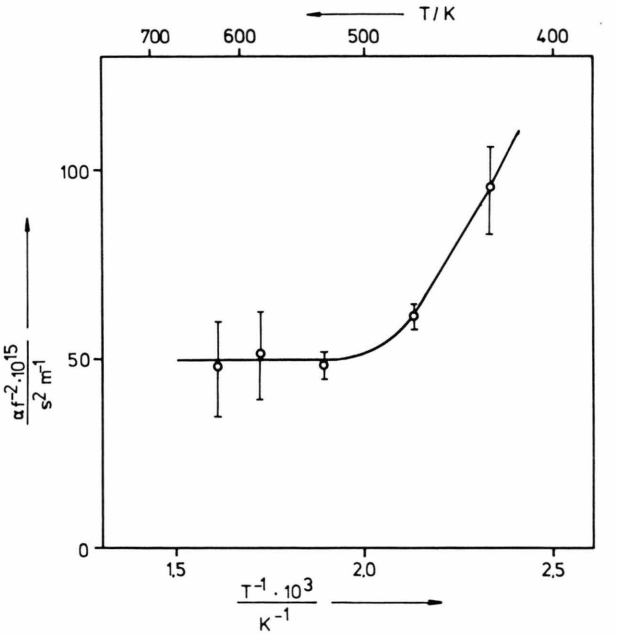

Fig. 6. $KNO_3 + AgNO_3$: Sound absorption coefficients as a function of the temperature at a molar fraction $x_{AgNO_3} = 0.6$ and 27.789 MHz.

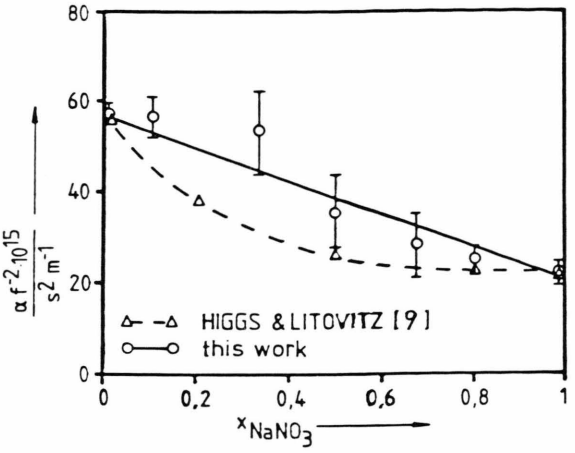

Fig. 7. $NaNO_3 + KNO_3$: Sound absorption coefficients as a function of the mole fraction of silver nitrate at 620 K and 27.789 MHz.

linear and equal. It may be described by the equation

$$u = a - b\,T_C\,,$$

where T_C is the temperature in °C. The coefficients a and b are also given in Table 1. The following values of the sound velocity in pure $NaNO_3$ can be found in the literature (temperature in °C, u in ms^{-1}):

Richards et al. [7] (1 MHz) $u = 2164 - 1.15\ T_C$,

Higgs and Litovitz [9] (55–125 MHz) $u = 2175 - 1.155\ T_C$,

Cerisier et al. [14] (100 kHz) $u = 2205.6 - 1.3975\ T_C + 4.2426 \cdot 10^{-4}\ T_C^2$,

Torell [15] (8 GHz) $u = 2166 - 1.1\ T_C$.

The values of the ultrasonic experiments agree very well with the value of this work, the difference being always below 0.5%. Except for the values of Cerisier [14] the ultrasonic velocity rises a bit from 1 MHz over 27 MHz and 55–125 MHz to the highest value measured by Torell [15] with Brillouin scattering experiments at a frequency of 8 GHz.

The ultrasonic velocity in pure silver nitrate is stated by

Higgs and Litovitz [9] $u = 1790.5 - 0.873\ T_C$,

Cerisier et al. [14] $u = 1915.6 - 1.8083\ T_C + 16.2024 \cdot 10^{-4}\ T_C^2$,

Torell [15] $u = 1850 - 0.97\ T_C$

(T_C in °C, u in ms^{-1}, same frequencies as above). The greatest deviation of 2% is found to the values of Higgs and Litovitz [9] at high temperatures. The hypersonic measurements of Torell [15] cannot be compared to the ultrasonic measurements.

$KNO_3 + AgNO_3$

The measured values of the ultrasonic velocities are summarized in Table 2. The curve is similar to the one of the $NaNO_3 + AgNO_3$ system. The temperature dependence is nearly linear so that in this system the equation $u = a - b\,T_C$ is also valid. The coefficients a and b are listed in Table 2.

For pure KNO_3 the following equations are found in the literature (temperature in °C, u in ms^{-1}, same frequencies as for pure $NaNO_3$):

Richards et al. [7] $u = 2157 - 1.194\ T_C$,

Higgs and Litovitz [9] $u = 2144 - 1.12\ T_C$,

Cerisier et al. [14] $u = 2278.4 - 1.6591\ T_C + 4.6856 \cdot 10^{-4}\ T_C^2$,

Torell [15] $u = 2342 - 1.45\ T_C$.

Table 1. $NaNO_3 + AgNO_3$: Sound velocity, measured values and coefficients of the balancing equation $u = a - b\,T_C$.

x_{AgNO_3}	Measured values u/ms^{-1}								Coefficients	
	T/K								a	b
	520	540	560	580	600	620	660	680	ms^{-1}	$ms^{-1}\,K^{-1}$
0.0	–	–	–	–	1794	1770	1724	1698	2510	1.19
0.1	–	–	–	–	1726	1701	1653	–	2454.3	1.214
0.2	–	–	–	–	1690	1665	–	–	2440	1.25
0.3	–	–	–	1680	1658	1631	–	–	2391.3	1.23
0.5	–	–	1640	1616	1590	1565	–	–	2343.2	1.26
0.6	–	1620	1598	1570	1543	1518	–	–	2320.9	1.3
0.8	–	1583	1560	1534	1510	1487	–	–	2236.6	1.21
0.9	1588	1563	1538	1512	1487	1462	–	–	2244.8	1.26
1.0	1565	1539	1515	1489	1465	1439	–	–	2216.9	1.25

Table 2. $KNO_3 + AgNO_3$: Sound velocity, measured values and coefficients of the balancing equation $u = a - b\,T_C$.

x_{AgNO_3}	Measured values u/ms^{-1}							Coefficients	
	T/K							a	b
	430	470	490	520	580	620	670	ms^{-1}	ms^{-1} K^{-1}
0.0	–	–	–	–	–	1751	1690	2512.6	1.23
0.2	–	–	–	–	1699	1653	–	2366	1.15
0.35	–	–	–	–	1649	1603	–	2316	1.15
0.5	–	–	1720	1685	1607	–	–	2339.5	1.26
0.6	1737	1696	1671	1637	1569	–	–	2223.6	1.13
0.8	–	–	1619	1585	1520	–	–	2156.4	1.1
1.0	–	–	–	1565	1489	–	–	2216.9	1.25

Table 3. $NaNO_3 + KNO_3$: Sound velocity, measured values and coefficients of the balancing equation $u = a - b\,T_C$.

x_{NaNO_3}	Measured values u/ms^{-1}					Coefficients	
	T/K					a	b
	540	575	590	620	660	ms^{-1}	ms^{-1} K^{-1}
0.0	–	–	–	1751	1701	2512.6	1.23
0.1	–	–	–	1749	1699	2524	1.25
0.33	–	1828	1807	1778	1726	2503.9	1.18
0.5	1890	1823	1801	1768	1723	2610.7	1.36
0.67	–	–	1785	1761	1718	2355.3	0.96
0.8	–	–	1810	1764	1727	2497.3	1.17
1.0	–	–	–	1770	1724	2510	1.19

The ultrasonic measurements again agree very well with this work. Similar to $NaNO_3$ and $AgNO_3$ these measurements show the tendency of a slightly rising ultrasonic velocity with rising frequency, where the measurements of Cerisier [14] are an exception.

$NaNO_3 + KNO_3$

The measured values for the ultrasonic velocity are given in Table 3. These values can be compared with the measurements of Higgs and Litovitz [9] and Cerisier et al. [16]. The values of Higgs and Litovitz show a good conformity. Both measurements find a maximum value of the ultrasonic velocity: Higgs and Litovitz at $x_{AgNO_3} = 0.2$ while ours at $x_{AgNO_3} = 0.3$. Cerisier et al. do not find a maximum value. The differences between the measurements amount to 30 ms^{-1}, or 2% in the middle of the composition interval.

The sound velocity of the three pure components has been measured by several authors at different frequencies. The fact that nearly nobody finds a dependence on frequency is due to the comparatively small variation used by each single author. But if one compares all five available measurements, ranging within five decades in frequency, one finds a clear rise of the ultrasonic velocity with rising frequency (Figure 8).

The reason for that may be interpreted as relaxational processes. From the theory of relaxation it can be deduced that the u^2 vs. $\log f$ curve has a point of inflection if the ultrasonic frequency is equal to the relaxation frequency [17]. With respect to the low number of measuring points the presentation in Fig. 9 might be a little too hypothetic. According to this, $AgNO_3$ and KNO_3 have relaxation times from 10^{-8} to 10^{-10} s whereas $NaNO_3$ has no relaxation time within the viewed frequency range, such a time should be smaller than 10^{-10} s.

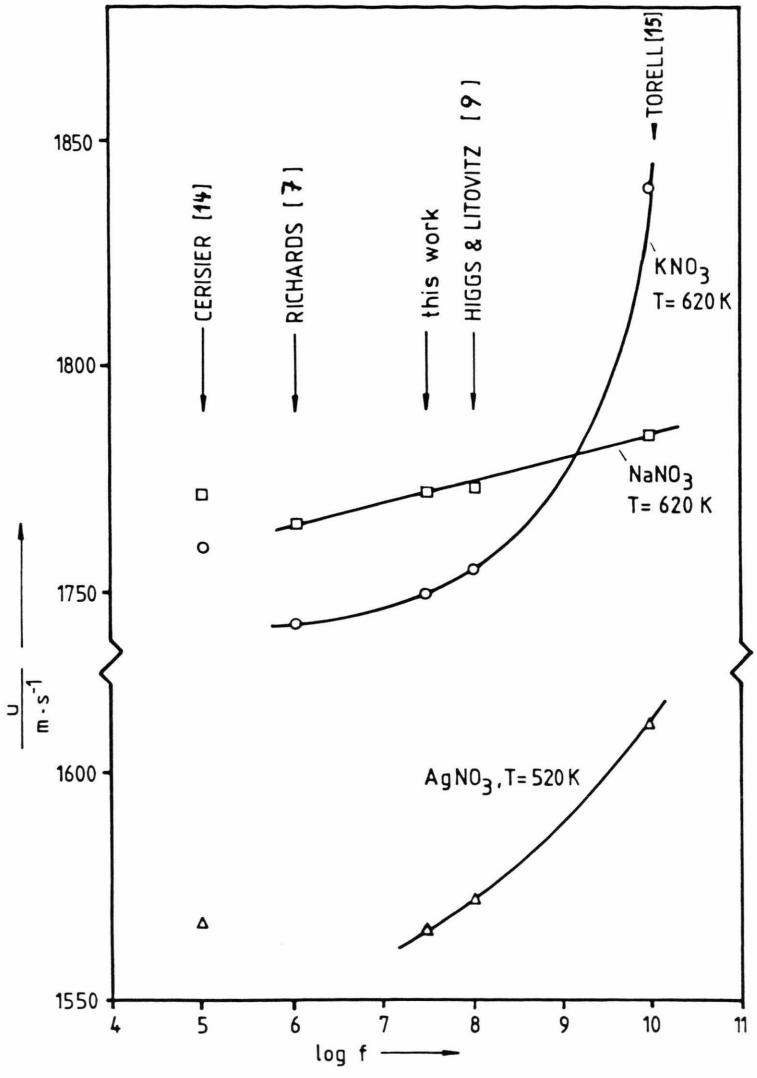

Fig. 8. $AgNO_3$, $NaNO_3$ and KNO_3: Sound velocity as a function of the frequency of the sound wave.

5. Thermodynamic Properties

From measurements of the sound velocity u some interesting thermodynamic properties can be calculated: the adiabatic constant $\gamma = \tilde{C}_p/\tilde{C}_v$ can be evaluated (cf. [3]) if the expansion coefficient α_v and the specific heat capacity at constant pressure $\tilde{C}_p$ are known

$$\gamma = \frac{\alpha_v^2 T u^2}{\tilde{C}_p} + 1, \tag{5}$$

the expansion coefficient being defined as

$$\alpha_v = -\frac{1}{\varrho_0}\left(\frac{\partial \varrho_0}{\partial T}\right)_p. \tag{6}$$

The densities of the $NaNO_3 + AgNO_3$ and $KNO_3 + AgNO_3$ systems were measured by Brillant [18] and have a nearly linear temperature dependence. For the calculation of the expansion coefficient in dependence of the temperature a linear regression was performed in the range of $(T \pm 30)$ K. The densities of the $NaNO_3 + KNO_3$ systems were measured by Murgulescu and Zuca [19]. For pure $NaNO_3$ they differ by only 0.5% from Brillant, and for pure KNO_3 by 0.6%. However, temperature dependences do not agree:

$NaNO_3$ (Brillant [18])	$d\varrho_0/dT = -0.75$ kg m^{-3} K^{-1},
$NaNO_3$ (Murgulescu [19])	$d\varrho_0/dT = -0.6$ kg m^{-3} K^{-1},

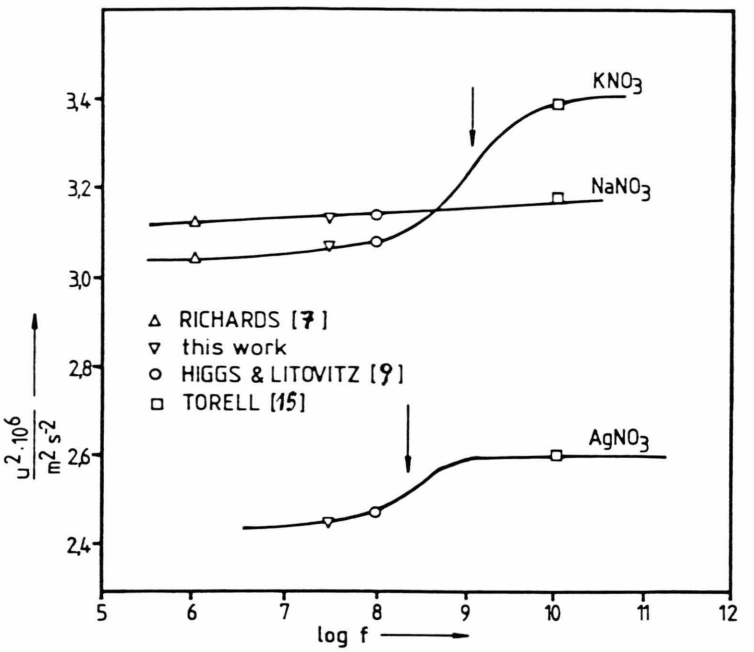

Fig. 9. Relaxation times of $AgNO_3$ and KNO_3 (↓).

KNO_3	$d\varrho_0/dT = -0.7$ kg m^{-3} K^{-1},
(Brillant [18])	
KNO_3	$d\varrho_0/dT = -0.6$ kg m^{-3} K^{-1},
(Murgulescu [19])	

a difference of 25% and 17%, respectively. For the calculation of the expansion coefficient the values of Brillant were taken. For the $NaNO_3 + KNO_3$ system a temperature dependence of $d\varrho_0/dT = -0.7$ kg m^{-3} K^{-1} was assumed. According to Murgulescu the density of this system is a linear function of composition and temperature. The intermediate values can be linearly interpolated.

The values of $\tilde{C}_p$ come from Gustafsson [20] and Gmelin [21]. As no composition dependent values were available, a linear relation of these values was assumed. According to Bockris and Richards [22] $\tilde{C}_p$ should be constant within ± 3% over a wide temperature interval, while this is contradictory to the values of Gustafsson [20].

The adiabatic compressibility χ_S is calculated by

$$\chi_S = 1/u^2 \varrho_0 \tag{7}$$

and the isothermal compressibility χ_T by

$$\chi_T = \chi_S \gamma \cdot \tag{8}$$

The values of γ, χ_S, and χ_T, calculated from the sound velocity, are shown in Tables 4 to 6. In the $NaNO_3 + AgNO_3$ and $NaNO + KNO_3$ systems the adiabatic constant γ is nearly a linear function of the mole fraction. In the $NaNO_3 + AgNO_3$ system γ decreases steadily, similar to the ultrasonic velocity, from $NaNO_3$ to $AgNO_3$. In the $KNO_3 + AgNO_3$ system γ has a significant maximum, due to the strong temperature dependence of the density from $x_{AgNO_3} = 0.2$ to 0.5. The temperature dependence of γ in all systems is small and positiv. The range is from 10^{-4} K^{-1} to $5 \cdot 10^{-4}$ K^{-1}. The adiabatic compressibility increases in all systems with rising temperature. The temperature dependence of all compositions is practically equal. Silver nitrate has the lowest compressibility of the investigated systems, potassium nitrate the highest. The difference between potassium and silver nitrate amounts to only 3%. The compressibility of all systems is a linear function of composition.

Rao [23] introduced into the discussion about the structure of the liquids the term

$$\mathbb{R} = \frac{1}{u}\left(\frac{\partial u}{\partial T}\right)_p \Big/ \frac{1}{V}\left(\frac{\partial V}{\partial T}\right)_p$$

Table 4. $NaNO_3 + AgNO_3$: Expansion coefficients, heat capacities, adiabatic constants, compressibilities and Rao's constant.

x_{AgNO_3}	T / K	$\alpha_v \cdot 10^4$ / K^{-1}	$\tilde{C}_p$ / $J\,kg^{-1}\,K^{-1}$	γ	$\tilde{C}_v$ / $J\,kg^{-1}\,K^{-1}$	$\chi_T \cdot 10^{10}$ / $s^2\,m\,kg^{-1}$	$\chi_S \cdot 10^{10}$ / $s^2\,m\,kg^{-1}$	$\mathbb{R}$
0.0	620	3.96	1609	1.189	1353	2.01	1.69	1.70
0.1	580	3.84	1530	1.171	1307	1.82	1.56	1.81
	620	3.88		1.177	1300	1.96	1.67	1.84
0.2	580	3.74	1451	1.164	1246	1.72	1.48	1.95
	620	3.79		1.171	1240	1.86	1.59	1.98
0.3	580	3.66	1372	1.159	1183	1.65	1.42	2.00
	620	3.70		1.164	1178	1.78	1.53	2.04
0.5	580	3.53	1214	1.155	1051	1.52	1.33	2.21
	620	3.58		1.160	1046	1.66	1.44	2.25
0.6	540	3.44	1135	1.147	989	1.40	1.22	2.33
	580	3.48		1.153	985	1.52	1.32	2.38
	620	3.53		1.157	981	1.66	1.43	2.43
0.8	540	3.13	977	1.136	860	1.29	1.14	2.44
	580	3.17		1.141	857	1.40	1.23	2.49
	620	3.21		1.145	853	1.51	1.32	2.53
0.9	540	2.96	898	1.129	795	1.25	1.10	2.72
	580	3.00		1.133	793	1.35	1.19	2.78
	620	3.04		1.136	790	1.47	1.29	2.83
1.0	540	2.81	819	1.124	729	1.21	1.08	2.89
	580	2.85		1.127	727	1.32	1.17	2.95
	620	2.88		1.130	725	1.43	1.27	3.02

Table 5. $KNO_3 + AgNO_3$: Expansion coefficients, heat capacities, adiabatic constants, compressibilities and Rao's constant.

x_{AgNO_3}	T / K	$\alpha_v \cdot 10^4$ / K^{-1}	$\tilde{C}_p$ / $J\,kg^{-1}\,K^{-1}$	γ	$\tilde{C}_v$ / $J\,kg^{-1}\,K^{-1}$	$\chi_T \cdot 10^{10}$ / $s^2\,m\,kg^{-1}$	$\chi_S \cdot 10^{10}$ / $s^2\,m\,kg^{-1}$	$\mathbb{R}$
0.0	620	3.74	1479	1.180	1254	2.06	1.74	1.86
0.2	580	4.12	1347	1.211	1112	1.89	1.56	1.64
	620	4.19		1.221	1103	2.04	1.67	1.66
0.35	580	4.19	1248	1.222	1021	1.81	1.48	1.66
	620	4.26		1.232	1013	1.96	1.59	1.68
0.5	530	3.72	1149	1.178	975	1.49	1.27	2.03
	580	3.86		1.194	962	1.67	1.40	2.03
	620	4.04		1.214	947	1.84	1.51	2.00
0.6	430	3.20	1083	1.123	965	1.19	1.06	2.03
	470	3.24		1.131	958	1.27	1.13	2.06
	530	3.50		1.158	935	1.45	1.25	1.99
	580	3.73		1.183	915	1.62	1.37	1.93
	620	3.93		1.205	898	1.77	1.47	1.89
0.8	530	3.10	951	1.133	839	1.32	1.17	2.25
	580	3.41		1.164	817	1.48	1.27	2.12
	620	3.67		1.191	798	1.63	1.37	2.03
1.0	530	2.82	819	1.124	729	1.19	1.06	2.86
	580	2.86		1.128	726	1.32	1.17	2.94
	620	2.89		1.131	724	1.43	1.27	3.01

Table 6. $NaNO_3 + KNO_3$: Expansion coefficients, heat capacities, adiabatic constants, compressibilities and Rao's constant.

x_{NaNO_3}	T / K	$\alpha_v \cdot 10^4$ / K^{-1}	$\tilde{C}_p$ / $J\,kg^{-1}\,K^{-1}$	γ	$\tilde{C}_v$ / $J\,kg^{-1}\,K^{-1}$	$\chi_T \cdot 10^{10}$ / $s^2\,m\,kg^{-1}$	$\chi_S \cdot 10^{10}$ / $s^2\,m\,kg^{-1}$	$\mathbb{R}$
0.0	620	3.74	1479	1.180	1254	2.07	1.75	1.91
0.1	620	3.76	1492	1.180	1265	2.07	1.76	1.90
0.33	570	3.74	1522	1.176	1294	1.85	1.57	1.72
	620	3.81		1.187	1282	2.01	1.69	1.74
0.5	570	3.78	1544	1.178	1310	1.84	1.56	1.96
	620	3.85		1.186	1302	2.03	1.71	2.00
0.67	570	3.82	1566	1.173	1335	1.89	1.61	1.39
	620	3.89		1.186	1321	2.04	1.72	1.40
0.8	620	3.92	1583	1.187	1333	2.03	1.71	1.69
1.0	620	3.96	1609	1.189	1353	2.02	1.70	1.70

with V the volume of the medium. He found that this term is 3.0 for many organic (mainly aromatic) liquids. The physical significance of this constant term is more or less unknown. For molten salts $\mathbb{R}$ is normally lower, the values range from 1.4 to 3.0 (Tables 4 to 6). For pure alkali halide melts Bockris and Richards [22] and Higgs and Litovitz [9] found Rao's constant to be between 1.5 and 2.0. Molten metals will have comparatively even lower values.

6. Volume Viscosity

The absorption coefficient (1) consists of three terms:

$$\alpha = \alpha_\eta + \alpha_{\eta_v} + \alpha_\lambda . \tag{9}$$

α_λ can be neglected as mentioned above. Then, according to (1) and (2):

$$\frac{\eta_v}{\eta} = \frac{4}{3}\left(\frac{\alpha}{\alpha_{class}} - 1\right). \tag{10}$$

We have calculated the classical absorption coefficient from the measured values of the ultrasonic velocity and the tabulated values of Janz [24] for the density and shear viscosity. If the values for density or shear viscosity were not stated, the values were inter- or extrapolated.

For the three binary systems $NaNO_3 + AgNO_3$, $KNO_3 + AgNO_3$ and $NaNO_3 + KNO_3$ the results are summarized in Table 7.

The volume viscosity of the $NaNO_3 + AgNO_3$ system is shown together with the shear viscosity in dependence on the composition at three different temperatures in Figure 10. A comparison of the concentration dependence of the volume viscosity in the three investigated systems to the absorption coefficients in Figs. 4, 6, and 7 shows that the curve of the ultrasonic absorption in dependence on composition is mainly ruled by η_v. The volume viscosity has a maximum value in the systems containing silver nitrate, which is shifted with decreasing temperature to the side of the alkali nitrate. The $NaNO_3 + KNO_3$ system shows a nearly ideal behavior within the error range, if one wants to denote a linear function of η_v in dependence on the mole fraction in this way.

The volume viscosity increases with decreasing temperature. The measurements on the $KNO_3 + AgNO_3$ system (Fig. 11) at a mole fraction $x_{AgNO_3} = 0.6$ show clearly that η_v at high temperatures has a lower temperature coefficient than η. The volume viscosity on the other hand increases near the melting point more steeply than the shear viscosity. For a better comparison, η_v and $10\,\eta$ are drawn in Figure 11.

Already the shapes of the absorption curves of water and the investigated molten salts are similar. Therefore it is not astonishing that also η_v has a strong similarity to the one of water: The temperature coefficients of η_v and α are negative.

According to Pinkerton [4] liquids can be divided into two groups:

1. Liquids with a positive temperature coefficient of the ultrasonic absorption and a relation of $\alpha/\alpha_{class} = 3$ to 400. Most (non associate) organic liquids

Table 7. Sound absorption coefficients, shear viscosity [24] and volume viscosity of the three systems $NaNO_3 + AgNO_3$, $KNO_3 + AgNO_3$, and $NaNO_3 + KNO_3$ at 620 K in dependence of the composition.

System	x_2	$\alpha f^{-2} \cdot 10^{15}$ / $s^2\,m^{-1}$	$\eta \cdot 10^3$ / $kg\,s^{-1}\,m^{-1}$	$\alpha_{\eta\,calc} f^{-2} \cdot 10^{15}$ / $s^2\,m^{-1}$	α / α_{class}	$\eta_v \cdot 10^3$ / $kg\,s^{-1}\,m^{-1}$
$NaNO_3 +$	0.0	23	2.43	6.1	3.7	8.7
$AgNO_3$	0.1	34	2.38	6.1	5.5	14.3
	0.3	47	2.32	5.7	8.2	22.3
	0.6	51	2.36	5.9	8.7	24.2
	0.8	45	2.29	5.4	8.4	22.6
	0.9	32	2.28	5.3	6.0	15.2
	1.0	26	2.27	5.3	4.9	11.8
$KNO_3 +$	0.0	57	2.75	7.2	7.9	25.3
$AgNO_3$	0.2	69	2.50	6.7	10.3	31.0
	0.35	72	2.37	6.2	11.6	33.5
	0.5	70	2.27	5.8	12.1	33.6
	0.6	48	2.26	5.7	8.4	22.3
	0.8	30	2.25	5.5	5.5	13.5
	1.0	26	2.27	5.3	4.9	11.8
$KNO_3 +$	0.0	57	2.76	7.3	7.8	25.1
$NaNO_3$	0.1	56	2.66	7.0	8.0	24.8
	0.33	53	2.46	6.2	8.6	24.9
	0.5	35	2.35	6.0	5.9	15.3
	0.67	28	2.33	6.0	4.7	11.5
	0.8	25	2.35	6.0	4.2	10.0
	1.0	23	2.45	6.2	3.7	8.8

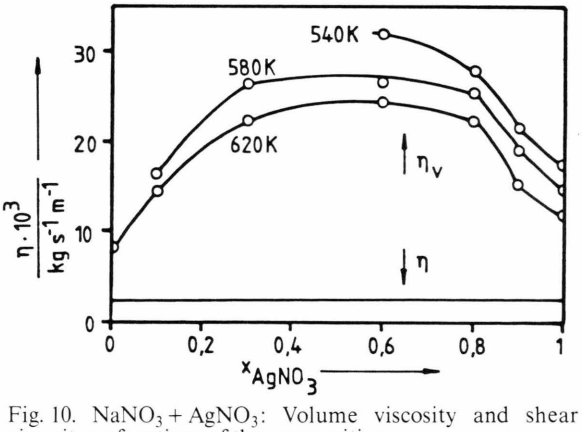

Fig. 10. $NaNO_3 + AgNO_3$: Volume viscosity and shear viscosity as functions of the composition.

belong to this group. According to Kneser [25] the strong sound absorption in these liquids can be referred to the slow energy exchange between inner and outer degrees of freedom.

2. Liquids with a negative temperature coefficient of the ultrasonic absorption and a relation of $\alpha/\alpha_{class} = 1$ to 3. All associated liquids like water, all alcohols [26], and the carbon acids, belong to this group. As reasons for volume viscosity in these liquids structural rearrangements are being discussed.

The molten salts take an intermediate position: on one hand the quotient α/α_{class} is greater than 3 (Table 7), on the other hand they belong with respect to the temperature coefficient to the associate liquids. Remarkable is also the similarity of the absorption curves of binary molten salts to those of water – alcohol mixtures. This suggests the conclusion that the reason for the volume viscosity in molten salts can be found in structural relaxation of the molecules. But the Arrhenius plots of the reduced absorption (α/f^2) in Fig. 6 and of the volume viscosity in Fig. 11 indicate that other loss mechanisms than structural relaxations are involved at higher temperatures.

Acknowledgement

We thank the Bundesminister für Forschung und Technologie, Bonn, for the financial support of this work.

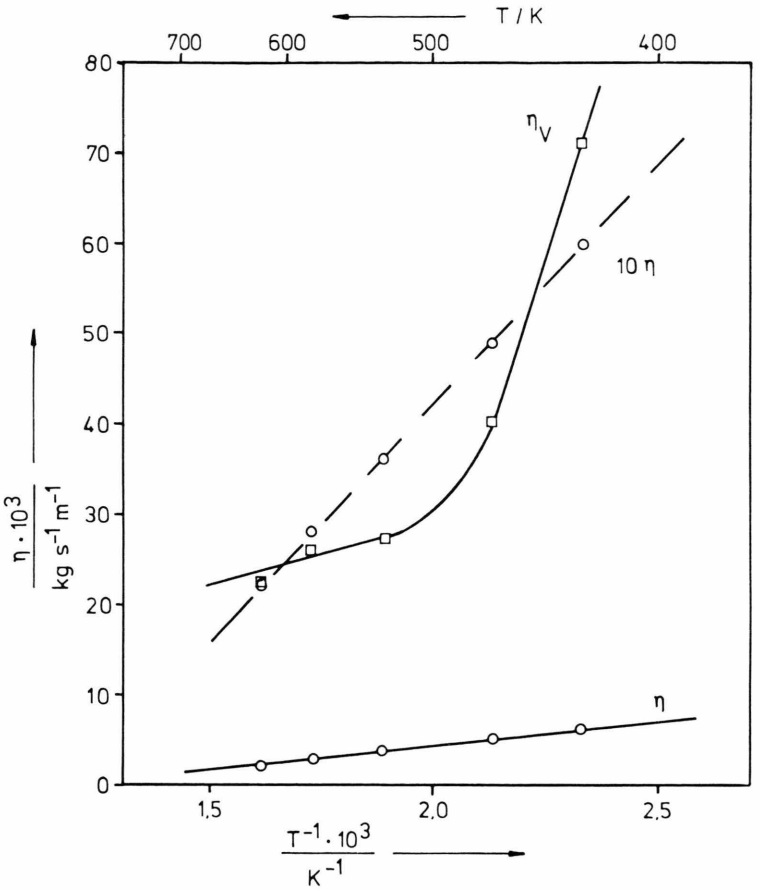

Fig. 11. $KNO_3 + AgNO_3$: Temperature dependence of shear and volume viscosity at a molar fraction of $x_{AgNO_3} = 0.6$.

[1] G. G. Stokes, Cambridge Transactions **8,** 287 (1845); **9,** Chapt. 49 (1851).
[2] G. Kirchhoff, Pogg. Ann. **134,** 177 (1868).
[3] S. R. De Groot and P. Mazur, Non-equilibrium Thermodynamics, North-Holland Publishing Company, Amsterdam 1962, Chapt. XII.
[4] J. M. M. Pinkerton, Proc. Phys. Soc. London **B 62,** 286 (1949).
[5] G. Busch and W. Maier, Z. Physik **137,** 494 (1954).
[6] J. H. Andreae, R. Bass, E. L. Heasell, and J. Lamb, Acustica **8,** 131 (1958).
[7] N. E. Richards, E. J. Brauner, and J. O'M. Bockris, Brit. J. Appl. Phys. **6,** 387 (1955).
[8] J. O'M. Bockris et al., Physico-Chemical Measurements at High Temperatures, Butterworths, London 1959.
[9] R. W. Higgs and T. A. Litovitz, J. Acoust. Soc. Amer. **32,** 1108 (1960).
[10] S. Sternberg and V. Vasilescu, Rev. Roum. Chimie **12,** 1187 (1967).
[11] J. Marchisio, G. Salvini, and Y. Doucet, J. Chimie Physique **70,** 1165 (1973).
[12] W. Fuchs, Thesis, Aachen 1982.
[13] G. Knape, Thesis, Göteborg 1975.
[14] P. Cerisier, G. Finiels, and Y. Doucet, J. Chimie Physique **71,** 836 (1974).
[15] L. Torell, Thesis, Göteborg 1975.
[16] P. Cerisier, G. Finiels, and Y. Doucet, J. Chimie Physique **72,** 895 (1975).
[17] W. Schaafs, Molekularakustik, Springer-Verlag, Berlin 1963.
[18] S. Brillant, J. Chimie Physique **65,** 2138 (1968).
[19] I. G. Murgulescu and S. Zuca, Rev. Roum. Chimie **2,** 227 (1959).
[20] S. E. Gustaffson, N.-O. Halling, and R. A. E. Tricklebank, Australian J. Chem. **18,** 1171 (1965).
[21] Gmelin, Handbuch der anorganischen Chemie, Band 61: Ag, Teil B1 (Verbindungen), Verlag Chemie, Weinheim 1971.
[22] J. O'M. Bockris and N. E. Richards, Proc. Roy. Soc. London **A 241,** 44 (1957).
[23] R. Rao, Indian J. Phys. **14,** 109 (1940); J. Chem. Phys. **9,** 682 (1941).
[24] G. J. Janz, U. Krebs, H. F. Siegenthaler, and R. P. T. Tomkins, J. Phys. Chem. Ref. Data **1,** 581 (1972).
[25] H. O. Kneser, Ann. Physik (5) **32,** 277 (1938).
[26] T. Kishimoto and O. Nomoto, J. Phys. Soc. Japan **9,** 620 (1954); **9,** 1021 (1954); **10,** 933 (1955).